

Figure S1 (Cai)

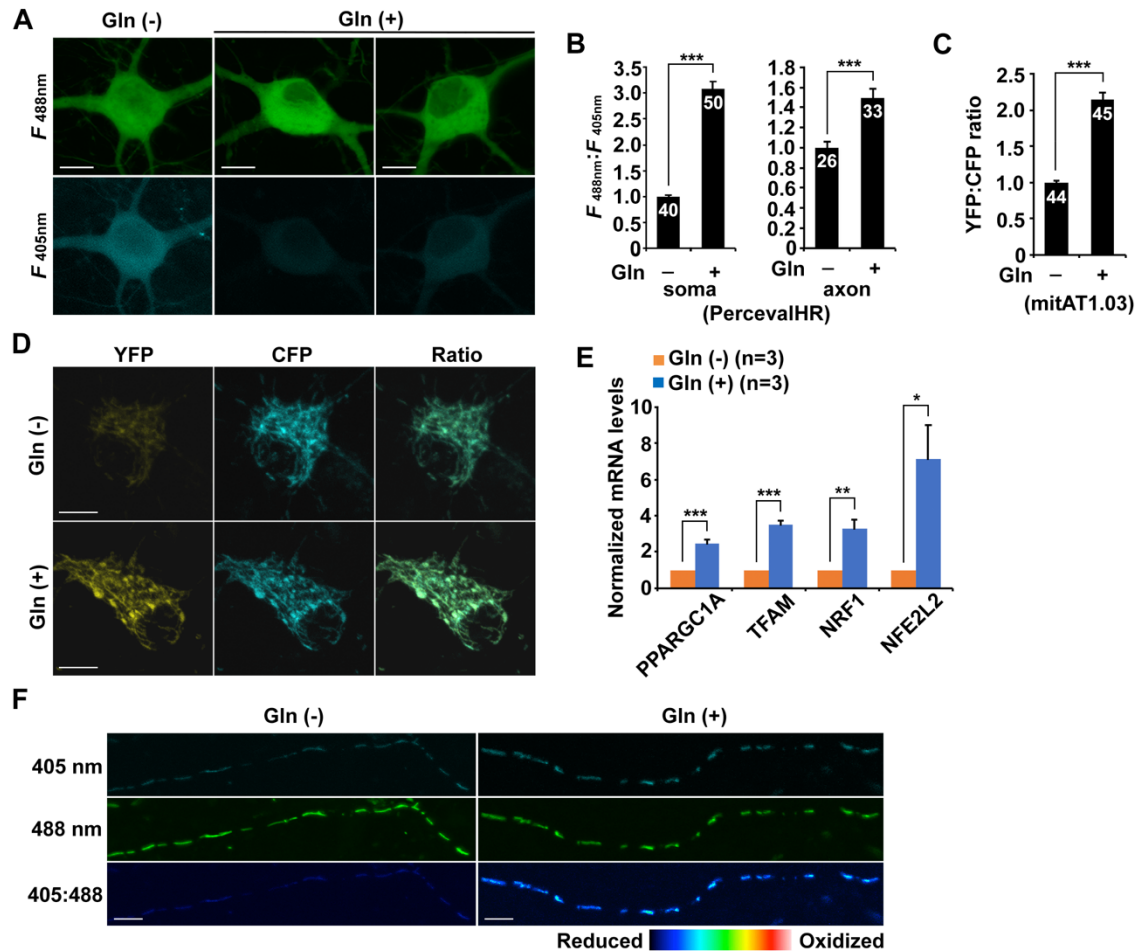


Figure S1. Increased cellular and mitochondrial ATP levels coupled with enhanced mitochondrial biogenesis in metabolically enhanced neurons. **(A-B)** Representative images **(A)** and quantitative analysis **(B)** showing that stimulating OXPHOS activity elevates ATP:ADP ratio in neurons expressing PercevalHR. The ATP:ADP ratios in the soma and the axon were normalized to those in control neurons without glutamine incubation, respectively **(B)**. **(C-D)** Glutamine metabolism markedly raised the healthy and active mitochondrial pool with high ATP levels as reflected by an increased YFP:CFP emission ratio on individual mitochondria in neurons expressing mitAT1.03 grown in the media with glutamine for 24 h. The YFP:CFP emission ratio of mitochondria in the soma of neurons in the presence of glutamine was normalized to that of control neurons in the absence of glutamine. **(E)** Increased mRNA levels of mitochondrial biogenesis genes in neurons under oxidation conditions.

The mRNA levels of PPARGC1A/PGC1 α , TFAM, NRF1 or NFE2L2 were normalized to GAPDH and to those of control neurons under the glycolytic condition. Data were quantified from three independent experiments. **(F)** Representative images showing an increase in oxidatively damaged mitochondria in axons treated with glutamine. The fluorescence of MitoROGFP was emitted at 510 nm and excited at 405 nm or 488 nm, respectively. Ratiometric images were generated from fluorescence excited by 405-nm light relative to that excited by 488-nm light. The ratio has been false colored with the indicated heat map, with high intensity indicative of ROGFP fluorescence in a more oxidative level. Data were quantified from a total number of neurons (n) indicated on the top of bars **(B and C)** from at least three independent experiments. Gln: glutamine. Scale bars: 10 μ m. Error bars: SEM. Student's *t* test: * p <0.05; ** p <0.01; *** p <0.001.

Figure S2 (Cai)

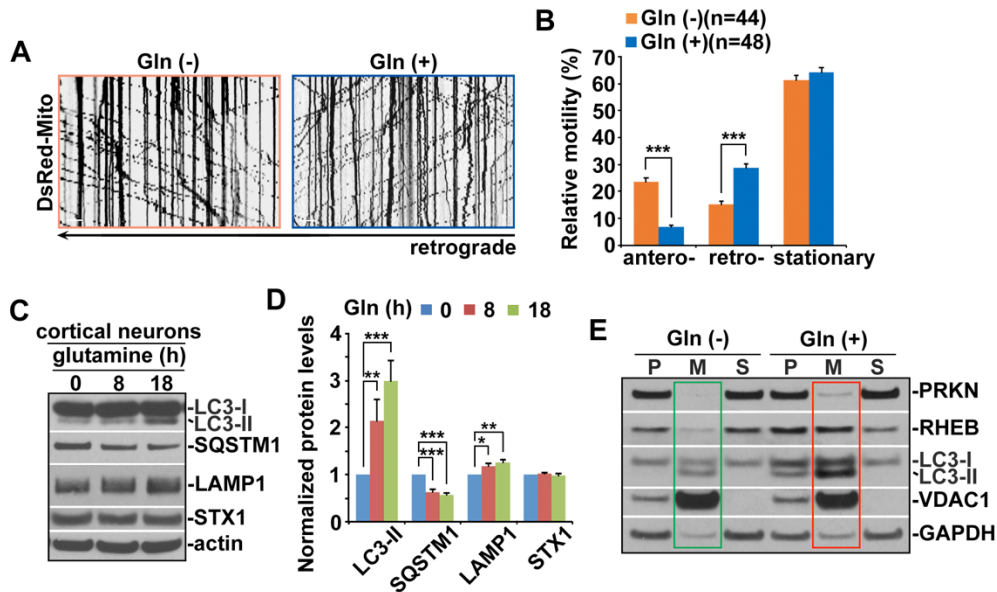


Figure S2. Altered mitochondrial axonal movement and mitophagy activation in neurons following OXPHOS stimulation. **(A-B)** Representative kymographs **(A)** and quantitative analysis **(B)** showing altered mitochondrial motility in axons under glutamine oxidation. Cortical neurons at DIV14-15 were treated with or without glutamine for 6 h, followed by 15 min time-lapse recordings. Vertical lines represent stationary organelles, oblique lines or curves to the right represent anterograde transport, and lines to the left indicate retrograde movement. Note that glutamine oxidation led to reduced anterograde transport and increased retrograde transport of axonal mitochondria, relative to neurons under the glycolytic condition. Relative mitochondrial motility was quantified from the number of neurons indicated in parentheses **(B)** from at least four independent experiments. **(C-D)** Mitophagy activation following incubation with glutamine for 8 h and 18 h. Cortical neuron lysates were solubilized, and equal amounts of protein (20 μ g) were loaded for sequential detection with antibodies on the same membrane after stripping between applications of each antibody as indicated. A neuronal marker STX1 (syntaxin 1) and actin were detected as loading controls, respectively. The intensities in neurons grown in the presence of glutamine for 8 h and 18 h were calibrated with actin levels and normalized to those in neurons in the absence of glutamine, respectively **(D)**. Data were quantified from four independent repeats. **(E)** Representative blots showing increased association of PRKN, RHEB, and LC3-II with mitochondria in neurons after stimulating OXPHOS activity. Neurons in the media with and without glutamine were subjected to fractionation into post-nuclear supernatant (P),

mitochondrial-enriched membrane fraction (M), and cytosolic supernatant (S). Equal amounts of protein (10 μ g) were sequentially immunoblotted with antibodies against PRKN/parkin, RHEB, LC3-II, VDAC1, and cytosolic protein GAPDH on the same membranes after stripping between each antibody application. Error bars: SEM. Student's *t* test: * p <0.05; ** p <0.01; *** p <0.001.

Figure S3 (Cai)

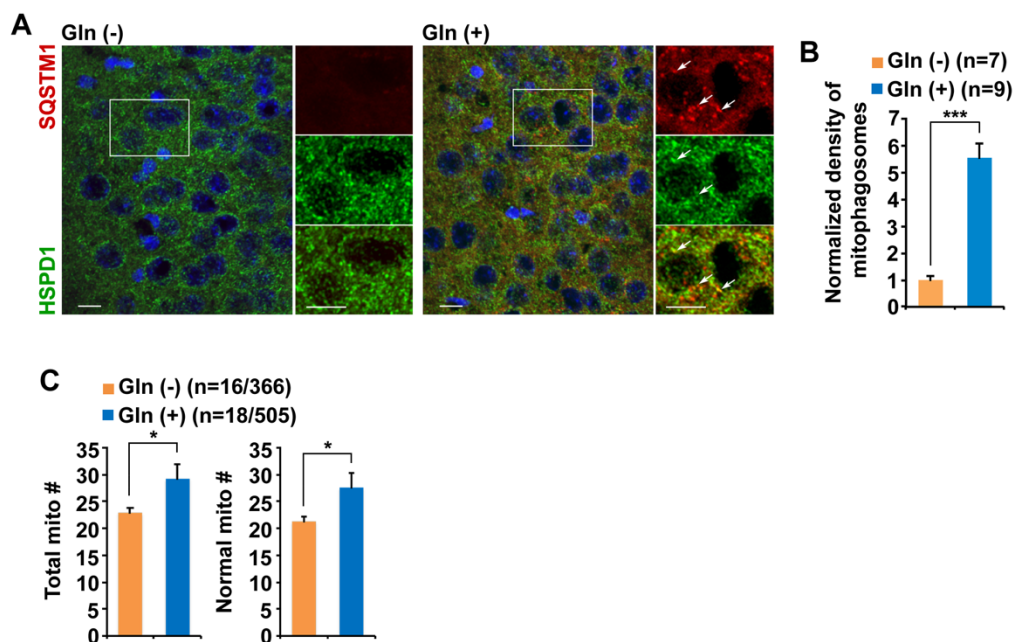


Figure S3. Mitophagy activation in mouse brains after glutamine supplementation. **(A-B)** An increase in the number of mitophagosomes co-labeled by antibodies against SQSTM1/p62 and HSPD1/HSP60 in the hippocampal CA3 regions of mouse brains under glutamine oxidation. Note that mitophagosomes were not readily observed in control mouse brains. The mean intensity of co-localized pixels that represent mitophagosomes was quantified and normalized to that of control mice supplemented with water. The density of mitophagosomes per section ($320 \mu\text{m} \times 320 \mu\text{m}$) was quantified from the total number of brain slice sections (n) indicated in parentheses **(B)** from three pairs of mice treated with and without glutamine. **(C)** Transmission electron microscopy (TEM) analysis showing increased numbers of total mitochondria and normal mitochondria in the soma of the hippocampal neurons in mouse brains supplemented with glutamine. Quantitative analysis was expressed as the numbers of total and morphologically normal mitochondria per neuronal perikaryal. Data were quantified from a total number of cells and mitochondria (n) indicated in parentheses. Scale bars: $10 \mu\text{m}$. Error bars: SEM. Student's t test: * $p < 0.05$; *** $p < 0.001$.

Figure S4 (Cai)

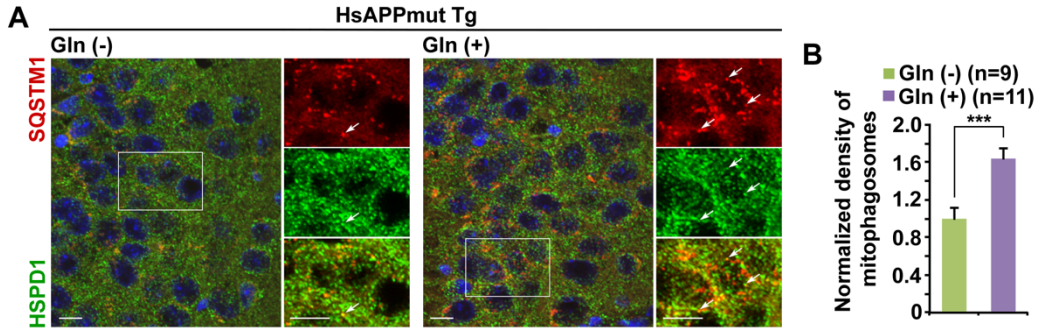


Figure S4. Mitophagy stress in AD-related mutant HsAPP Tg mouse brains upon stimulation of energetic activity. **(A)** Representative images **(A)** and quantitative analysis **(B)** showing that mitophagosome accumulation was intensified in the hippocampal neurons of mutant HsAPP Tg mouse brains following glutamine supplementation. The densities of mitophagosomes co-labeled by antibodies against SQSTM1 and HSPD1 in the hippocampal CA3 regions per section ($320\ \mu\text{m} \times 320\ \mu\text{m}$) were quantified and normalized to that of control mice fed with water from the total number of brain slice sections (n) indicated in parentheses **(B)** and from three pairs of mutant HsAPP Tg mice in the presence and absence of glutamine treatment, respectively. Scale bars: $10\ \mu\text{m}$. Error bars: SEM. Student's t test: $***p < 0.001$.

Figure S5 (Cai)

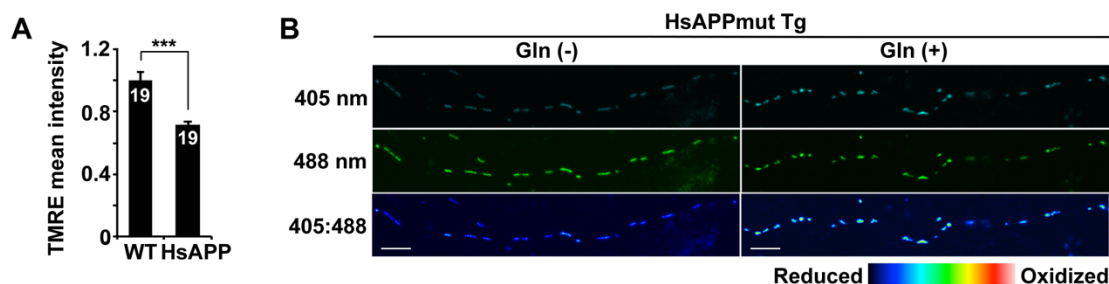


Figure S5. Augmentation of oxidized mitochondrial retention in AD axons under glutamine oxidation. **(A)** Depolarization of mitochondrial membrane potential ($\Delta\psi_m$) in mutant HsAPP neurons under basal conditions. Note that mutant HsAPP neurons displayed reduced mean intensity of TMRE fluorescence as compared to that of neurons from WT littermate controls. Cortical neurons transfected with mitochondrial marker CFP-Mito were loaded with $\Delta\psi_m$ -dependent dye TMRE for 30 min prior to imaging. The mean intensity of TMRE in the soma of mutant HsAPP neurons was normalized to that in the neurons from WT littermate controls. Data were quantified from a total number of neurons indicated on the top of bars from more than three independent repeats. **(B)** Marked increases in oxidized mitochondria along the axons of AD neurons incubated with glutamine. The fluorescence of MitoROGFP was emitted at 510 nm and excited at 405 nm or 488 nm, respectively. Ratiometric images were generated from fluorescence excited by 405-nm light relative to that excited by 488-nm light. The ratio has been false colored with the indicated heat map, with high intensity indicative of ROGFP fluorescence in a more oxidative environment. Scale bars: 10 μ m. Error bars: SEM. Student's *t* test: *** $p < 0.001$.

Figure S6 (Cai)

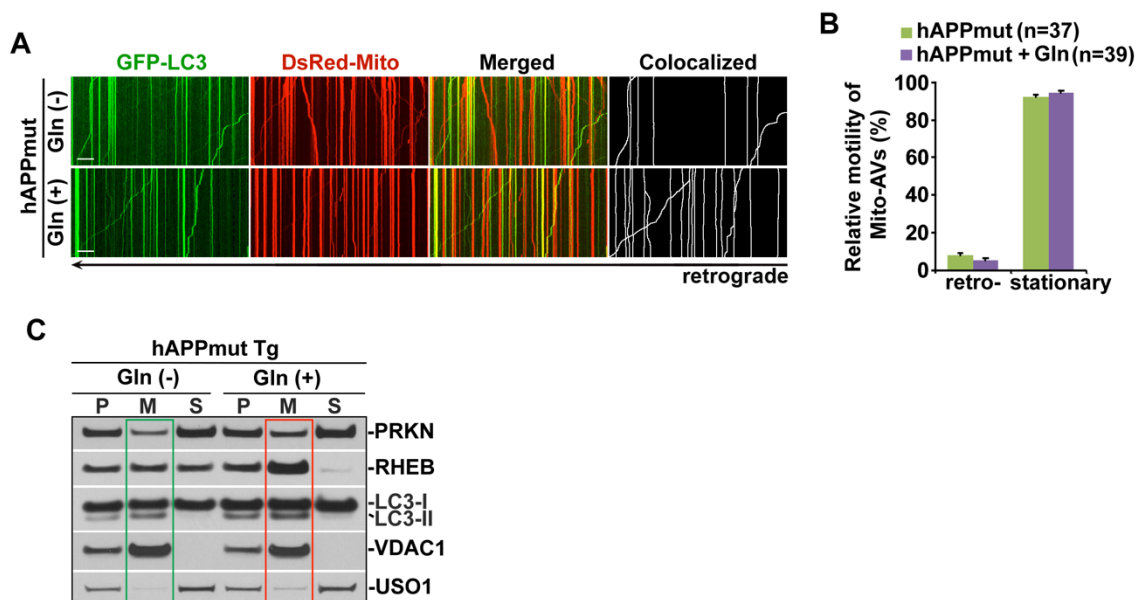


Figure S6. Impeded retrograde transport of mitophagosomes in AD axons with and without glutamine incubation. **(A-B)** Representative dual-channel kymographs **(A)** and quantitative analysis **(B)** showing that retrograde movement of mitophagosomes co-labeled by GFP-LC3 and DsRed-Mito was halted in mutant HsAPP Tg axons in the presence and absence of glutamine. The relative motility of mitophagosomes in AD axons with and without glutamine treatment was quantified, respectively. Data were quantified from the total number of neurons indicated in parentheses **(B)** from three independent repeats. **(C)** Representative blots showing that glutamine treatment augmented the levels of PRKN, RHEB, and LC3-II in mitochondrial fractions purified from mutant HsAPP Tg neurons. Scale bars: 10 μ m. Error bars: SEM. Student's *t* test.

Figure S7 (Cai)

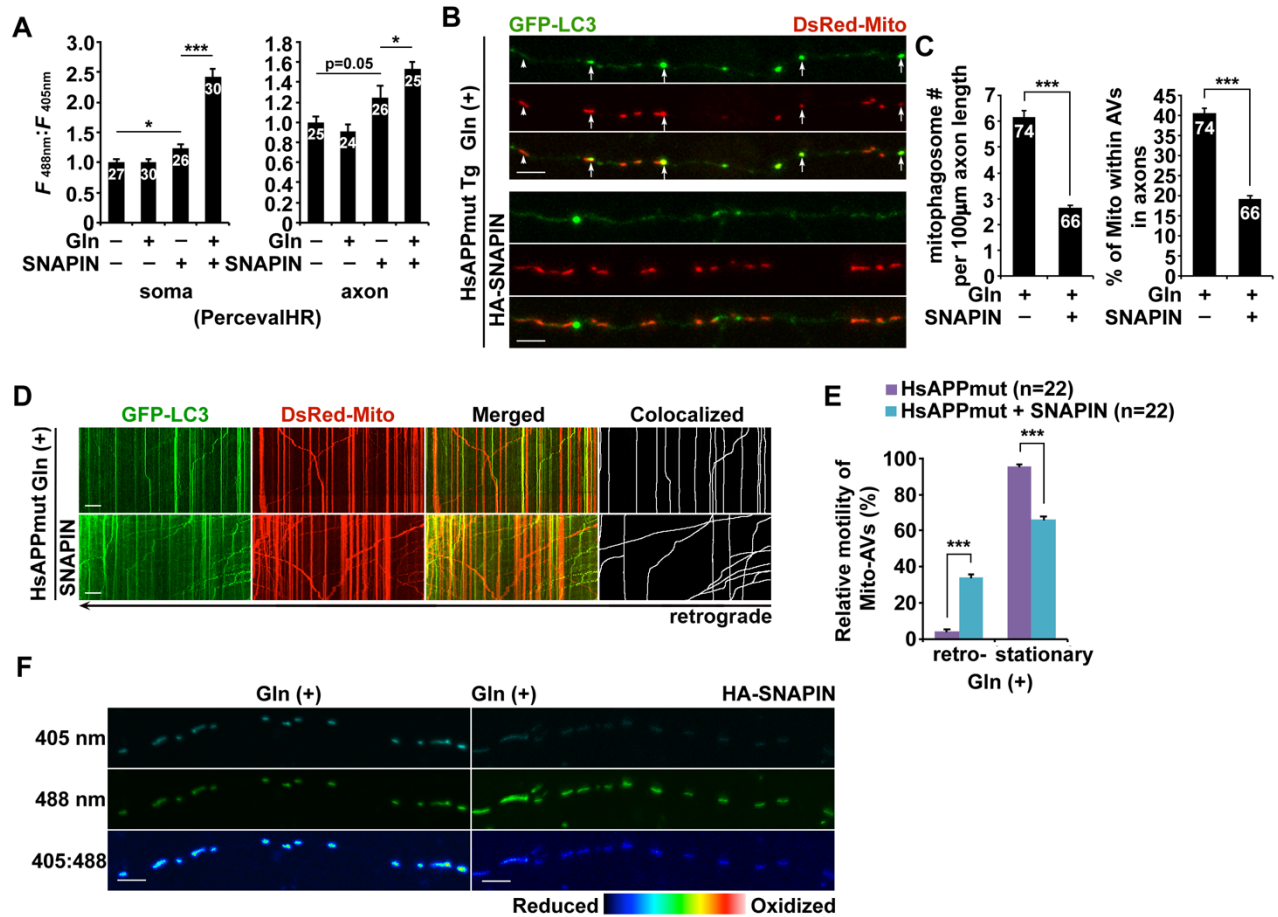


Figure S7. Energetic stimulation corrects bioenergetic deficiency and attenuates mitophagy stress in AD axons with increasing SNAPIN levels. **(A)** SNAPIN elevation increased cellular ATP levels in mutant HsAPP Tg neurons grown in media with glutamine. The ATP:ADP ratio in the soma and the axon of AD neurons were normalized to those in vector-expressed control AD neurons without glutamine incubation, respectively. Data were quantified from the number of neurons indicated on the top of bars from more than three independent repeats. **(B-C)** Representative images **(B)** and quantification **(C)** showing that glutamine treatment ameliorated mitophagosome accumulation with mutant HsAPP axons with overexpression of SNAPIN. The number of mitophagosomes per 100 μm axon and the percentage of mitochondria within autophagic vacuoles (AVs) along mutant HsAPP Tg axons with and without SNAPIN elevation were quantified, respectively **(C)**. **(D-E)** Overexpression of SNAPIN restored impaired retrograde transport of mitophagosomes in AD axons under glutamine

oxidation. The relative motility of mitophagosomes in mutant HsAPP axons with and without increasing SNAPIN was quantified, respectively (**E**). (**F**) Representative images showing that mutant HsAPP axons with elevated SNAPIN expression exhibited decreased oxidative stress of mitochondria in the presence of glutamine. Data were quantified from the number of neurons indicated on the top of the bars (**A**, **C**) or in parentheses (**E**) from more than three independent repeats. Scale bars: 10 μm . Error bars: SEM. Student's *t* test: * $p < 0.05$; *** $p < 0.001$.

Figure S8 (Cai)

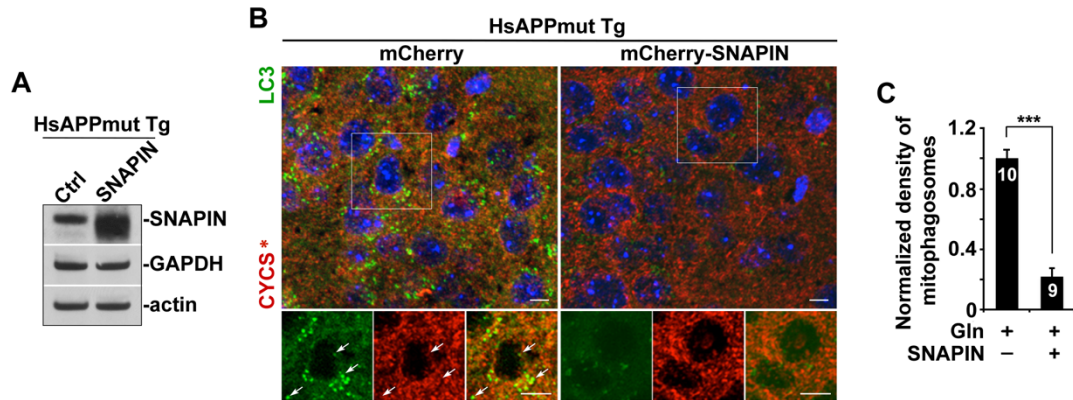


Figure S8. Increasing SNAPIN levels enhances mitophagic clearance in AD mouse brains supplemented with glutamine. **(A)** Elevated SNAPIN expression in the hippocampus of mutant HsAPP Tg mouse brains after AAV injection. A total of 10 μ g of hippocampal homogenates from mutant HsAPP mouse brains transduced with AAV-mCherry or AAV-mCherry-SNAPIN were sequentially immunoblotted on the same membrane after stripping between each antibody application. **(B-C)** Overexpression of SNAPIN alleviated mitophagy stress in the hippocampal neurons of AD mouse brains under glutamine metabolism. Note a marked reduction of mitophagosomes (white arrows) in the soma of hippocampal neurons in mutant HsAPP Tg mouse brains injected with AAV-mCherry-SNAPIN as compared to that in the control AD mice expressing AAV-mCherry. CYCS*: color is converted from blue to red for better contrast **(B)**. Data were quantified from a total number of brain slices sections (n) indicated on the top of bars **(C)** from two pairs of mutant HsAPP Tg mice with AAV injection. Scale bars: 10 μ m. Error bars represent SEM. Student's *t* test: *** $p < 0.001$.